

1  
2  
3  
4  
5  
6  
7  
8  
9  
10  
11  
12  
13  
14

**Development of a Stable and Sustainable Environmental Energy Source for Continuous Thermal-to-Electric Energy Conversion Utilizing the Effect of Acceleration Forces Causing Internal Voltage Gradients**

Kuo Tso Chen

OPTROMAX Co. Taiwan, Zhudong Township, Hsinchu County 310658, Taiwan (R.O.C.)

**CORRESPONDING AUTHOR**

E-mail: gtchen0@gmail.com.

Phone: +886-918-629-588

15 **ABSTRACT**

16 The second law of thermodynamics is widely viewed as unbreakable, with past attempts to refute  
17 it consistently proven wrong. However, in 2015, the author recognized that gravity gives  
18 molecular motion a directional component, suggesting that a setup involving gravity or a  
19 centrifugal force might transcend the randomness-based framework of the second law. By 2021,  
20 it was speculated that high-altitude plasmas could have this effect, and by April 2022,  
21 electrolytes with ions of differing masses might exhibit the same phenomenon. This hypothesis  
22 was experimentally confirmed in August 2022. In November 2024, the author discovered that  
23 Tolman observed electromotive force (EMF) in electrolytes under centrifugal and gravitational  
24 fields as early as 1910—a result that precisely matches these findings. Strangely, no one had  
25 previously linked Tolman’s findings to a potential challenge of the second law.

26 As Tolman reported in 1916, metals produce only minor potential differences in a gravitational  
27 field, unlike ionic solutions. Thus, if an ionic liquid column’s top and bottom are connected with  
28 a metal in a gravitational field, the metal’s negligible potential difference allows the ionic  
29 solution’s potential to induce a current, generating electrical energy. Although this current  
30 temporarily stops when the electrolyte loses equilibrium, thermal vibrations push molecules back  
31 to equilibrium, reestablishing the potential difference and renewing the current—thus converting  
32 thermal energy to electrical energy without needing a temperature difference.

33 We validate this process through theoretical derivation and experiments, which demonstrate that  
34 this energy output is stable and sustained over time.

35

36

## 37 1. INTRODUCTION

38 In today's energy landscape, addressing global warming and finding effective energy  
39 conversion methods are critical challenges. Many energy systems rely on converting thermal  
40 energy into mechanical or electrical energy. However, according to the Carnot theorem<sup>1</sup>, once  
41 heat is transferred from a high-temperature region to a low-temperature region and loses its  
42 temperature gradient, the thermal energy can no longer be converted into usable energy.

43 The second law of thermodynamics<sup>2</sup> is considered an unbreakable iron law. Historically,  
44 any claims of violating this law have been proven incorrect<sup>3</sup>. However, we believe that there may  
45 still be a possibility to transcend this law. In 2015, the author of this paper realized that  
46 gravitational force gives molecular motion directionality rather than being entirely random,  
47 suggesting that a setup involving gravity or centrifugal force could surpass the second law of  
48 thermodynamics, which is based on random motion. By 2021, it was hypothesized that plasmas  
49 in the upper atmosphere might exhibit such properties. In April 2022, electrolytic solutions were  
50 also noted to contain charged particles of different masses, which might exhibit the same  
51 phenomenon. After experiments were conducted, this hypothesis was confirmed in August 2022.  
52 Later, in November 2024, the author discovered that Tolman experimentally demonstrated the  
53 existence of an electromotive force (EMF) in electrolytes under centrifugal and gravitational  
54 fields as early as 1910<sup>4</sup>, which aligns precisely with the author's experimental findings.  
55 However, it is intriguing why, for over a century, no one identified Tolman's conclusions as a  
56 means to surpass the limitations of the second law of thermodynamics.

57 Simply put, as Tolman concluded in 1916, the potential difference produced by metals in  
58 a gravitational field is far smaller than that of ionic solutions<sup>5</sup>. Therefore, in a gravitational field,  
59 if the top and bottom of an ionic liquid column are connected by a metal, the metal's potential

60 difference is negligible, and the potential difference between the top and bottom of the ionic  
61 liquid column will induce a current within the metal, allowing it to output electrical energy. After  
62 generating a current, the electrolyte deviates from equilibrium due to electron exchange, causing  
63 the current to stop. However, the 'thermal energy' driving 'thermal vibrations' will diffuse the  
64 molecules back toward equilibrium, reestablishing the potential difference and producing the  
65 next current. Thus, thermal energy is converted to electrical energy without requiring a  
66 temperature difference, effectively transcending the second law of thermodynamics.

67         This phenomenon was investigated by Colley (1882), who examined its impact on  
68 electrolytes and demonstrated that acceleration could directly affect current flow in such  
69 materials<sup>6</sup>. Des Coudres (1892) extended these studies, noting the centrifugal effects on  
70 electrolytes, which provided further insight into the role of acceleration in ion movement<sup>7</sup>. These  
71 early studies laid the foundation for understanding how ions, owing to their larger mass than that  
72 of electrons, could exhibit distinctive behaviors under acceleration, particularly in electrolyte  
73 systems. Subsequent practical applications of this phenomenon have been widely studied. For  
74 example, in 2011, L. Lao, C. Ramshaw, and H. Yeung conducted research on enhancing the  
75 process of water electrolysis in a centrifugal acceleration field<sup>8</sup>.

76         While this phenomenon has been widely studied, there has been little research on its  
77 potential to break the thermal energy conversion limits and convert heat into electrical energy  
78 without relying on a temperature gradient. The scientific community has largely adhered to the  
79 second law of thermodynamics, rarely considering this possibility.

80         To validate this concept, we begin by theoretically exploring how thermal energy can be  
81 converted into electrical energy. Our derivation shows that, during the acceleration process, the  
82 voltage difference induced by this phenomenon not only exists on the surface of the material but

83 is also distributed evenly throughout the interior of the conductor. This finding offers new insight  
84 into the phenomenon of internal voltage differences and lays the foundation for future theoretical  
85 innovations. Through theoretical derivation, we found that when the pH of an electrolyte is close  
86 to 7, even a small difference in ion concentration can cause significant changes in pH. This can  
87 lead to a large voltage difference with only slight changes in height or distance along the  
88 centrifugal force direction. Adjusting the pH could therefore offer a way to significantly increase  
89 the electrical output efficiency. Furthermore, we conducted experiments to measure stable, long-  
90 term current output. While the observed energy output is small, this initial validation from a  
91 theoretical perspective demonstrates that, with appropriate engineering optimization, this method  
92 could lead to a thermoelectric conversion system with economic feasibility for specific  
93 applications.

94         Consider a rotating system: if the rotation speed is doubled, the centrifugal force  
95 increases fourfold, meaning that only a quarter of the original distance is required to generate the  
96 same voltage difference. By connecting four such systems in series, the total voltage difference  
97 could reach four times the original value. Given that, under the same cross-sectional area, the  
98 resistance of the conductor is proportional to its thickness, the resistance at a quarter of the  
99 original distance would be one-fourth of the original value. Thus, the energy output from each  
100 system would be four times greater. The four systems can be placed in the same space. From  
101 this, it can be inferred that such a design could significantly increase the energy output efficiency  
102 by up to 16 times, whereas the air resistance energy consumption would only increase by  
103 approximately four times. Therefore, increasing the rotational speed could lead to the generation  
104 of practically usable electrical energy.

105 In conclusion, while energy cannot be created from nothing, high-energy electrons are  
106 more likely to cross material interfaces in an accelerating field, facilitating current flow. As these  
107 high-energy electrons move through the material, the generation of electrical energy inevitably  
108 accompanies the dissipation of kinetic energy, akin to the dissipation of heat. Further theoretical  
109 development will explain how thermal vibrational energy drives charged particles to overcome  
110 gravitational or centrifugal forces, replenishing regions depleted by voltage differences or across  
111 conductive interfaces. Since the system can maintain energy exchange under sustained  
112 acceleration, even in the absence of a temperature gradient, this process could transcend the  
113 limitations of the Carnot theorem, offering the potential to continuously convert ambient thermal  
114 energy into usable electrical energy.

115

## 116 **2. MATERIALS AND METHODS**

117 To verify our hypothesis, we designed a structure resembling a battery in which positive  
118 and negative ions with different masses experience different forces in a centrifugal or  
119 gravitational field. This results in a potential difference at the terminals, and we measured  
120 whether this potential difference could provide a stable and long-term energy output. The  
121 fabrication and testing of the gravity battery involved several key steps, with each main  
122 experimental stage detailing the materials and equipment used, along with the rationale behind  
123 their selection.

124 1. *Electrode Preparation:* A titanium electrode plate (1 mm thick, 99.5% pure) was  
125 selected for its stability and was coated with a 1  $\mu\text{m}$  thick layer of platinum on  
126 both sides through electroplating. This platinum coating not only minimizes  
127 potential differences but also renders the electrode inert, significantly reducing the

128 likelihood of chemical reactions with the electrolyte in the gravity battery. The  
129 platinum-coated titanium sheet was then cut into circular electrodes with a  
130 diameter of 50 mm via a water jet to ensure low temperatures during the cutting  
131 process, thereby preserving the physical and chemical properties of the electrode  
132 surface.

133 2. *Cavity Formation:* Multiple silicone sheets, each with an outer diameter of 60 mm  
134 and an inner diameter of 40 mm, were used to form cavities for the gravity battery  
135 units. Silicone was chosen as the cavity material because of its chemical inertness,  
136 which prevents any reaction with ions in the electrolyte.

137 3. *Electrolyte Solution:* A potassium chloride solution (99.9% pure) was prepared  
138 with the pH adjusted to near neutrality ( $\text{pH} \approx 7$ ) to serve as the electrolyte.  
139 Potassium chloride was selected because the net weights of chloride and  
140 potassium ions in water, after accounting for buoyancy, significantly differ,  
141 enhancing the system's response. Additionally, setting the pH close to 7 allows  
142 for achieving the maximum potential difference with minimal ion concentration  
143 changes. These aspects will be discussed in detail later in the article.

144 4. *Battery Assembly:* The materials described above were used to assemble two  
145 gravity battery packs, each consisting of six small gravity cells electrically  
146 connected in series. The electrode spacings within the cells were set at 2 mm, 4  
147 mm, 8 mm, 16 mm, 24 mm, and 32 mm. Arranging multiple cells with varying  
148 electrode spacings allows any significant reaction in one of the cells to be easily  
149 detected and measured, ensuring reliable data collection across different spacing  
150 conditions.

- 151 5. *External Connections and Housing:* Copper sheets (99% pure) were employed for  
152 external electrical connections because of their relatively low resistance, which  
153 helps minimize measurement deviations caused by external resistance and  
154 improves overall measurement accuracy. The assembled gravity battery was  
155 housed in a 304 stainless steel casing and sealed with epoxy resin to ensure  
156 stability during testing. Stainless steel was chosen for its high strength and  
157 chemical inertness, preventing deformation under high gravity or centrifugal  
158 forces and ensuring that it would not corrode or degrade over prolonged  
159 measurements.
- 160 6. *Centrifuge Testing Setup:* The battery pack was placed in a centrifuge with a  
161 rotation radius of 1200 mm, and the centrifuge was accelerated to generate a  
162 centrifugal force equivalent to 10 times the gravitational force at the Earth's  
163 surface (10G). The large rotation radius was selected to ensure that the direction  
164 of the centrifugal force remained precisely vertical across different parts of the  
165 electrodes, whereas high acceleration was chosen to amplify the voltage, making  
166 it easier to measure.
- 167 7. *Voltage Measurement During Centrifugation:* Voltage and time data were  
168 recorded via an MMV-387SD three-channel voltage data recorder (Lutron, Sunwe  
169 Co., Taiwan) with a resolution of 0.1 mV.
- 170 8. *Long-term Stability Test:* The gravity battery was oriented in a forward position  
171 with an output impedance of 6.8 M $\Omega$  and monitored over a period of 55 days.  
172 This setup was intended to verify that the generated voltage could persist over an  
173 extended duration with power output, confirming that it was not merely a



174 transient phenomenon. Voltage measurements were taken via a Keysight 34465A  
175 digital multimeter (Keysight Technologies, Santa Rosa, CA, United States) with a  
176 resolution of 0.1  $\mu\text{V}$ .

177 9. *Inverted Position Test:* The gravity battery was then inverted (placed upside  
178 down) and subjected to a similar long-term test over 86 days, with voltage  
179 readings taken via the same Keysight multimeter setup. This was done to confirm  
180 that the voltage was indeed caused by gravitational acceleration, with the  
181 hypothesis that reversing the direction of gravity would result in an opposite  
182 voltage. Therefore, the sample was inverted for measurement.

183

184

## 185 **2.1. Theoretical derivation process**

186

### 187 *2.1.1. Self-Generated Potential Difference of Plasma in a Gravity Field*

188 The phenomenon of decreasing air density with increasing altitude on the Earth's surface  
189 is well known. Therefore, for a simple composition of gases, the concentration at higher altitudes  
190 is lower than that at lower altitudes. Specifically, the variation in the concentration of a pure gas  
191 with height, when in equilibrium, follows the Boltzmann distribution.<sup>9</sup> The relationship is  
192 described by Equation (1).

$$193 \frac{C_{h+\Delta h}}{C_h} = e^{-\frac{\varepsilon_{h+\Delta h} - \varepsilon_h}{kT}} = e^{-\frac{mG\Delta h}{kT}} \quad \dots \dots \dots \quad (1)$$

194 where  $h$  is the height coordinate value,  $C_h$  is the concentration of ions at height  $h$ ,  $C_{h+\Delta h}$  is the  
195 concentration of ions at height  $h + \Delta h$ ,  $\varepsilon_h$  is the potential energy of the ion at height  $h$ ,  $\varepsilon_{h+\Delta h}$  is  
196 the potential energy of the ion at height  $h + \Delta h$ ,  $m$  is the mass of the particle (or ion),  $G$  is

197 gravity,  $mG$  is the gravitational force on the particle (or ion), and  $kT$  is the product of the  
 198 Boltzmann constant  $k = 1.380649 \times 10^{-23} \text{ J/K}^{10}$  and the thermodynamic temperature  $T$ .

199 Applying the same principle, considering a plasma medium that is either fully ionized or  
 200 nearly fully ionized, in the presence of gravity but in the absence of an electric field, when in  
 201 equilibrium, the distribution of ions inside the plasma with height will be as shown in Equation  
 202 (2).

$$203 \frac{C_{h+\Delta h}}{C_h} \Big|_{E=0} = e^{-\frac{\varepsilon_{h+\Delta h} - \varepsilon_h}{kT}} \Big|_{E=0} = e^{-\frac{mG\Delta h}{kT}} \Big|_{E=0} \dots \dots \dots (2)$$

204 where  $E$  is the electric field.

205 Notably, Equations (1) and (2) contain a mass variable  $m$ , meaning that heavier particles  
 206 will experience a greater change in concentration with height than lighter particles. Thus, in the  
 207 absence of an electric field, ions with larger masses are subjected to greater gravitational forces,  
 208 resulting in a larger concentration difference between high and low positions. In contrast, in the  
 209 absence of an electric field, ions with smaller masses experience weaker gravitational forces,  
 210 leading to a smaller concentration difference. Therefore, as seen from Equation (2), in the  
 211 absence of an electric field and when the masses of positive and negative ions in the plasma are  
 212 different, the lower region will have a greater number of heavier ions than lighter ions, whereas  
 213 the upper region will have a greater number of lighter ions than heavier ions. For example, in  
 214  $Li^+$  and  $Cl^-$  plasmas, the mass of  $Cl^-$  is approximately 5 times greater than that of  $Li^+$ , so the  
 215 gravitational force of  $Cl^-$  is also approximately 5 times greater than that of  $Li^+$ . When the  
 216 number of positive and negative ions is the same, on the basis of equation (2) and the  
 217 abovementioned principles, in the absence of an electric field, the number of chloride ions  $Cl^-$   
 218 will be greater than the number of lithium ions  $Li^+$  in the lower region of the plasma, resulting in  
 219 a negative charge. In the upper region, the number of chloride ions  $Cl^-$  is less than that of

220 lithium ions  $Li^+$ , resulting in a positive charge. When the electricity above the plasma is positive  
 221 and the electricity below it is negative, a top-down electric field is generated. This electric field  
 222 causes  $Cl^-$  to move upward and  $Li^+$  to move downward, reducing the difference in charge  
 223 between the upper and lower parts. The rates of change of positive ions and negative ions in the  
 224 plasma change with height are the same, on the basis of charge balance. That is, when charge  
 225 balance is achieved, apart from the uppermost and lowermost regions, the intermediate area  
 226 remains electrically neutral. In the case of charge balance, when the residual electric field  
 227 strength is  $E$ , equation (3) can be obtained by adding the electric field term  $E$  to the Boltzmann  
 228 distribution<sup>9</sup> in equation (2), and equation (4) can be derived from equation (3):

$$229 \frac{C_{Li^+(h+\Delta h)}}{C_{Li^+(h)}} = e^{-\frac{(m_{Li^+}G+qE)\Delta h}{kT}} = \frac{C_{Cl^-(h+\Delta h)}}{C_{Cl^-(h)}} = e^{-\frac{(m_{Cl^-}G-qE)\Delta h}{kT}} \quad \dots \dots \dots \quad (3)$$

$$230 m_{Li^+}G + qE = m_{Cl^-}G - qE$$

$$231 E = \frac{(m_{Cl^-}-m_{Li^+})G}{2q} \quad \dots \dots \dots \quad (4)$$

232 where  $C_{Li^+(h)}$  is the concentration of  $Li^+$  at height  $h$ ,  $C_{Li^+(h+\Delta h)}$  is the concentration of  $Li^+$ s at  
 233 height  $h + \Delta h$ ,  $m_{Li^+}$  is the mass of  $Li^+$ ,  $E$  is the electric field inside the plasma and is positive in  
 234 the downward direction,  $G$  is gravity and is positive in the downward direction,  $C_{Cl^-(h)}$  is the  
 235 concentration of  $Cl^-$  at height  $h$ ,  $C_{Cl^-(h+\Delta h)}$  is the concentration of  $Cl^-$ s at height  $h + \Delta h$ ,  $m_{Cl^-}$   
 236 is the mass of  $Cl^-$ , and  $q$  represents the charge of the negative electron, which is  
 237  $1.602176634 \times 10^{-19}C$ .<sup>10</sup>

238 Importantly, the electric field in equation (4) exists within the plasma body. This means  
 239 that charge accumulation occurs at the upper and lower surfaces and that there is no charge  
 240 accumulation inside the plasma; however, an electric field is distributed throughout the entire

241 plasma body rather than being confined to its surface. In other words, gravity or a centrifugal  
242 force generates an electric field within the conductor (plasma).

243 Another noteworthy point is that Tolman's 1910 experiment demonstrated that increasing  
244 the concentration of iodide ions had minimal impact on the voltage generated in a centrifugal  
245 field. This aligns with our derived Equation (4), which indicates that the electric field in plasmas  
246 or conductors depends solely on the individual masses of the ions <sup>4</sup>, and is independent of ion  
247 concentration.

248 When the height difference from top to bottom is H, the voltage difference  $\nabla V$  can be  
249 obtained as shown in equation (5):

250 
$$\nabla V = \frac{(m_{Cl^-} - m_{Li^+})GH}{2q} \dots \dots \dots \quad (5)$$

251 Equations (4) and (5) indicate that whenever the masses of the positive and negative charge  
252 carriers in the plasma are different, an electric field will spontaneously form inside the plasma  
253 body under the influence of gravitational or centrifugal forces. This extends the effect of  
254 acceleration forces, causing internal voltage differences<sup>4</sup> by expanding the electric field from the  
255 surface of the conductor to its interior.

256

257 *2.1.2. Illustrate the energy conversion mechanism*

258 Currently, the plasma formed by lithium ions and electrons is widely used in many  
259 applications. Using the same derivation and calculations, equation (4) can be expanded to  
260 equation (6):

261 
$$E = \frac{(m_- - m_+)G}{2q} \dots \dots \dots \quad (6)$$

262 where  $m_+$  represents the mass of positively charged particles in the plasma and where  $m_-$   
263 represents the mass of negatively charged particles. In lithium plasma, the positively charged

264 particles are lithium ions with a mass of  $1.157 \times 10^{-26}\text{kg}^{11}$ , whereas the negatively charged  
 265 particles are electrons with a mass of  $9.109 \times 10^{-31}\text{kg}^{12}$ . Since the mass of lithium ions is  
 266 significantly greater than that of electrons, equation (6) can be simplified to equation (7).

$$267 \quad E_{in.Li+.plasma} \cong -\frac{m_{Li+G}}{2q} \dots \dots \dots \quad (7)$$

268 Equation (7) shows that owing to the mass difference between lithium ions and electrons, the  
 269 electric field required to maintain plasma neutrality is not zero. This means that in the presence  
 270 of a gravitational or centrifugal field, a nonzero electric field exists within the lithium plasma.  
 271 Next, by considering a plasma formed by potassium ions and electrons and following the same  
 272 approach as in the previous example with lithium ions, we obtain equation (8).

$$273 \quad E_{in.K+.plasma} \cong -\frac{m_{K+G}}{2q} \dots \dots \dots \quad (8)$$

274 Notably, when equations (7) and (8) are compared, the mass of potassium ions, approximately  
 275  $6.492 \times 10^{-26}\text{kg}^{11}$ , is much greater than that of lithium ions, which is  $1.157 \times 10^{-26}\text{kg}^{11}$ . This  
 276 causes the electric field formed within the potassium ion plasma in the same gravitational or  
 277 centrifugal field to be significantly stronger than that formed within the lithium ion plasma. This  
 278 also leads to a much greater potential change within the potassium-ion plasma than in the  
 279 lithium-ion plasma over the same distance along the direction of the force field. Consider the  
 280 structure shown in Fig. 1. On the left is a chamber with lithium ion plasma in an insulator, and on  
 281 the right is a chamber with potassium ion plasma in an insulator. Each chamber is connected by a  
 282 conductor at a height difference of  $h$ . From the previous derivation, we know that because the  
 283 electric fields in the two plasmas differ under gravity, the potential differences at the same height  
 284 also differ. If the voltage difference between the conductor ends below is zero, we can find the  
 285 potential difference of the upper conductor, as shown in equation (9).

286

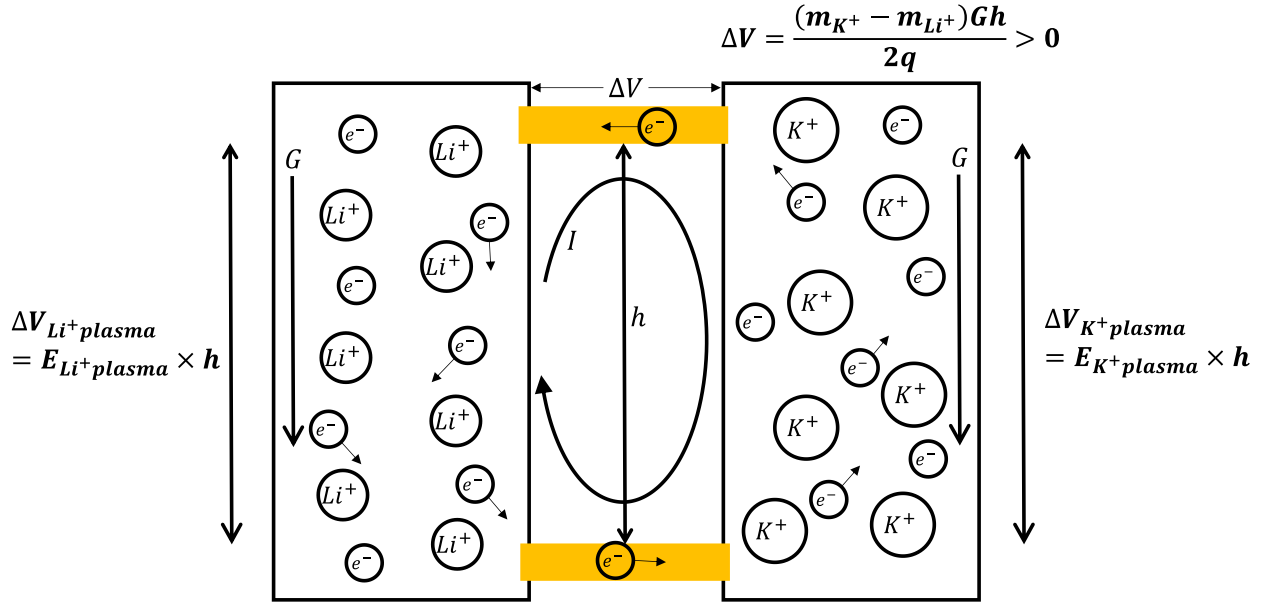


**Fig. 1.** Two adjacent chambers are under the influence of a gravitational field, with one containing lithium ion plasma and the other containing potassium ion plasma. Electrical connections are made at the top and bottom of each chamber, showing a schematic representation of the spontaneously generated current within the system.

287

288 
$$\Delta V = E_{Li^+plasma} \times h - E_{K^+plasma} \times h = \frac{(m_{K^+} - m_{Li^+})Gh}{2q} > 0 \dots \dots \dots (9)$$

289 Equation (9) shows that because the masses of potassium ions and lithium ions are different, a  
 290 potential difference forms across the upper conductor. The voltage on the side near the lithium  
 291 plasma is higher than that near the potassium plasma. When a potential difference forms across  
 292 the conductor, a spontaneous current flows to balance it. This creates an electron flow from the  
 293 potassium plasma to the lithium plasma, or equivalently, a current from the lithium plasma to the  
 294 potassium plasma. Owing to this electron flow, the upper part of the potassium plasma loses  
 295 electrons, lowering its concentration below equilibrium. This causes electrons in the potassium  
 296 plasma to diffuse upward due to thermal motion. In the lithium-ion plasma, an electron

297 concentration higher than the equilibrium level in the upper region causes electrons to diffuse  
 298 downward. On the basis of charge balance, spontaneous electron flow occurs from the lithium  
 299 plasma to the potassium plasma in the lower conductor. Thus, a spontaneous circulating current  
 300 forms in this structure, following the clockwise direction in the figure. Notably, the energy for  
 301 this electron diffusion comes from thermal energy, whereas the circulating current is electrical  
 302 energy. Thus, thermal energy is converted into electrical energy. In other words, two parallel,  
 303 different plasma bodies spontaneously generate a circulating current that converts thermal energy  
 304 into electrical energy. This heat-to-electricity conversion without a temperature difference goes  
 305 beyond the Carnot Theorem<sup>1</sup> (published by Nicolas Léonard Sadi Carnot in 1820). It surpasses  
 306 the second law of thermodynamics<sup>2</sup>.

307

308 *2.1.3. The energy that can be output by a self-generated electric field is*

309 If electrodes are placed at high or low positions, a potential difference occurs between the  
 310 upper and lower electrodes according to equation (5), and Ohm's law<sup>13</sup> indicates that this  
 311 potential difference can output a current  $I$  in equation (10).

312 
$$I = \frac{\nabla V}{R_{wire} + R_{plasma}} \quad \dots \dots \dots \quad (10)$$

313 where  $\nabla V$  is the voltage difference between the two electrodes before connecting the wire,  $R_{wire}$   
 314 is the resistance of the wire, and  $R_{plasma}$  is the resistance of the plasma.

315 In the process of generating electrical energy, when  $N$  hot ions, atoms, and molecules  
 316 acquire  $N$  electrons from one of the electrodes, they transfer  $N$  electrons to the other electrode  
 317 from other  $N$  hot ions, atoms, and molecules and transfer  $Nq\nabla V$  of thermal energy into electrical  
 318 energy during the electron exchange process. These electron exchanges can cause the  
 319 concentration or ratio of ions, electrons, or molecules in the plasma near the electrode to deviate

320 from equilibrium. However, thermal vibrations and molecular diffusion also lead to electron  
 321 exchange among other atoms and ions, which restores equilibrium and re-establishes the  
 322 potential difference. In this way, the output, along with the internal electrical energy of the  
 323 plasma, can continue with a power P, as shown in equation (11):

$$324 \quad P = \frac{(\nabla V)^2}{R_{wire} + R_{plasma}} \quad \dots \dots \dots \quad (11)$$

325         Owing to the conservation of energy, the temperature of the plasma will be reduced while  
 326 electrical energy is output. Therefore, the thermal energy supplies the energy for thermal  
 327 vibrations, which drive diffusion processes. As diffusion progresses toward equilibrium, it re-  
 328 establishes the potential difference, allowing electrical energy to be generated. In this way,  
 329 thermal energy is ultimately converted into electrical energy.

330

331 *2.1.4. Example Calculation of the Plasma Self-Generated Electric Field and Voltage under*  
 332 *Gravity*

333         To better illustrate the concept discussed, we provide an example calculation for  
 334 determining the voltage difference generated by a plasma system under gravity. Taking the  
 335 structure in Figure 1 as an example, with the parameter values listed in Table 1, we can derive  
 336 the following results from Equations (7), (8), and (9): the self-generated electric field inside the  
 337 potassium ion plasma is approximately -1.9870 μV/m, and the self-generated electric field inside  
 338 the lithium ion plasma is approximately -0.35408 μV/m. When the height difference *h* is one m,  
 339 the self-generated voltage difference is 1.6329 μV. Referring to Equation (11), we can obtain the  
 340 maximum output power as shown in Equation (12), where  $R_{wire}$  represents the resistance of the  
 341 wire and where  $R_{plasma}$  represents the total resistance of the plasma.



Parameter	Symbol	Value
Mass of lithium ion <sup>11,12</sup>	$m_{Li^+}$	$1.157 \times 10^{-26} kg$
Mass of potassium ion <sup>11,12</sup>	$m_{K^+}$	$6.492 \times 10^{-26} kg$
Gravitational acceleration <sup>14</sup>	$G$	$9.80665 m/s^2$
Elementary charge <sup>10</sup>	$q$	$1.602176634 \times 10^{-19} C$

**Table 1.** Relevant parameters for lithium ion (Li<sup>+</sup>) plasma and potassium ion (K<sup>+</sup>) plasma,

where the mass of lithium ions is  $m_{Li^+} = 6.9675 \times 1.66054 \times 10^{-27} kg = 1.157 \times 10^{-26} kg$ ,<sup>11,12</sup> and the mass of potassium ions is  $m_{K^+} = 39.0983 \times 1.66054 \times 10^{-27} kg = 6.492 \times 10^{-26} kg$ .<sup>11,12</sup>

342

343 
$$P_{plasma.Li^++plasma.K^+} = \frac{2.6663 \times 10^{-12} V^2}{R_{wire} + R_{plasma}} > 0 \quad \dots \dots \dots$$

344 (12)

345 The power is generated mainly by the exchange of electrons under thermal vibration and  
346 the diffusion transport of ions and molecules.

347 Although the output energy is very low, under energy conservation, gravity can convert  
348 thermal energy into electrical energy when there is no temperature difference in the entire  
349 system, which violates the limitations of Carnot's theorem,<sup>1</sup> which states that the maximum  
350 energy output rate of a heat engine cannot be greater than the temperature difference divided by  
351 the absolute temperature.

352

353 *2.1.5. Changes in the Ion Concentrations of Ionic Aqueous Solutions in the Gravity Field*

354 The previous paragraph used plasma as a theoretical deduction. However, ion plasma  
355 requires high temperatures and is difficult to control and operate; however, at normal  
356 temperatures, ions can be found in aqueous solutions. Considering an ionic aqueous solution,

357 when the net masses or mass–charge ratios of positive and negative ions in water (the weight of  
 358 the ions minus the buoyancy force of the water on the ions) are different, a potential difference  
 359 can also be generated by gravity. As demonstrated in Tolman's 1910 experiment, the offset  
 360 voltage of a lithium iodide aqueous solution under a specific rotational speed (approximately 70  
 361 units) was about  $4.3 \text{ mV}^4$ , whereas the offset voltage of a potassium iodide aqueous solution  
 362 under the same rotational speed (and thus the same centrifugal force) was about  $3.5 \text{ mV}^4$ ,  
 363 showing a significant difference. If a setup similar to Fig. 1 is used, with one side replaced by a  
 364 lithium iodide aqueous solution instead of lithium plasma, and the other side by a potassium  
 365 iodide aqueous solution instead of potassium plasma, a similar voltage difference and  
 366 thermoelectric conversion effect can be achieved.

367 Next, we employ a configuration with one side being an electrolyte aqueous solution and  
 368 the other side a copper conductive plate as the basis for calculations and experiments. As Tolman  
 369 mentioned in his 1916 paper, the offset voltage in metals under the same acceleration is  
 370 significantly smaller than that in ionic liquids<sup>5</sup>, suggesting that a similar effect should also be  
 371 achievable.

372 For example, potassium chloride aqueous solution was used. Because chloride ions and  
 373 potassium ions are both strong electrolytes, they are almost completely dissociated. Owing to the  
 374 effect of gravity, the potential energy of the ions changes, causing the ion concentration to  
 375 change with height. The concentrations of chloride ions and potassium ions change with height  
 376 due to the potential energy difference caused by gravity. According to Boltzmann's distribution  
 377 law,<sup>9</sup> the concentration changes with height in the steady state without convection can be  
 378 obtained as shown in equations (13) and (14):

$$379 \quad [C_{K^+}]_h = [C_{K^+}]_0 e^{-\frac{m_{K^+} \cdot net \cdot Gh}{kT}} \quad \dots \dots \dots \quad (13)$$

380  $[C_{Cl^-}]_h = [C_{Cl^-}]_0 e^{-\frac{m_{Cl^-.net} Gh}{kT}} \dots \dots \dots$  (14)

381 where  $h$  is the height coordinate value,  $[C_{K^+}]_h$  is the potassium ion concentration at height  $h$ ,  
 382  $[C_{K^+}]_0$  is the potassium ion concentration at height 0,  $m_{K^+.net}$  is the net effective mass of  
 383 potassium ions after accounting for buoyant force in water,  $[C_{Cl^-}]_h$  is the chloride ion  
 384 concentration at height  $h$ ,  $[C_{Cl^-}]_0$  is the chloride ion concentration at height 0, and  $m_{Cl^-.net}$  is the  
 385 net effective mass of chloride ions after accounting for buoyant force in water.

386 When calculating the net mass of an ion, the buoyant force exerted by water on the ion  
 387 must be subtracted from the mass of the ion. To determine this buoyant force, the effective  
 388 volume of the ion is first calculated. This volume is then multiplied by the density of water to  
 389 obtain the buoyant force acting on the ion. A KCl aqueous solution with a concentration of 2 N  
 390 was used as an example.

391

392 *2.1.5.1. Calculation of the effective volume of chloride ( $Cl^-$ ) ions*

393 Because the volume of hydrogen ions is close to zero, the volume of an HCl unit (one  
 394 hydrogen ion plus one chloride ion) is approximately equal to the volume of chloride ions. When  
 395 calculating the volume of the HCl unit, first, equation (15) is considered:

396  $V_{HCl+1kgH_2O} = [1000g + N \times W_{mol.HCl}] / d_{HCl+1kgH_2O} \dots \dots \dots$  (15)

397 where  $V_{HCl+1kgH_2O}$  is the volume of HCl dissolved in one kilogram of water,  $N$  is the mole  
 398 number of solute,  $W_{mol.HCl} = (35.446 + 35.457)/2 + (1.00784 + 1.00811)/2 = 36.459 g^{11}$   
 399 is the mass of the HCl in one mole, and  $d_{HCl+1kgH_2O}$  is the density of the aqueous solution of  
 400 HCl dissolved in one kilogram of water. The values of the parameters used to calculate the  
 401 effective volume of chloride ( $Cl^-$ ) ions are summarized in Table 2.

402

Parameter	Symbol	Value
Mass of HCl in one mole <sup>11</sup>	$W_{mol.HCl}$	36.459 g
Density of the solution after 2 N HCl is dissolved in one kilogram of water at 25°C, <sup>15</sup>	$d_{HCl(2N)+1kgH_2O}$	1.03008 g/cm <sup>3</sup>
Density of the solution after 1.8 N HCl is dissolved in one kilogram of water at 25°C. <sup>15</sup>	$d_{HCl(1.8N)+1kgH_2O}$	1.02690 g/cm <sup>3</sup>
Volume of the solution after 2 N HCl is dissolved in one kilogram of water at 25°C. ( $V = W/d$ )	$V_{HCl(2N)+1kgH_2O}$	1041.587 cm <sup>3</sup>
Volume of the solution after 1.8 N HCl is dissolved in one kilogram of water at 25°C. ( $V = W/d$ )	$V_{HCl(1.8N)+1kgH_2O}$	1037.621 cm <sup>3</sup>
Effective volume of 0.2 mole $H^+$ + 0.2 mole $Cl^-$ in a 2 N HCl solution	$0.2(V_{H^+(2N)} + V_{Cl^-(2N)})$	3.966 cm <sup>3</sup>
Effective volume of 1 mol hydrogen ions	$V_{H^+(2N)}$	$\cong 0$
Effective volume of 1 mol chloride ions	$V_{Cl^-(2N)}$	19.83 cm <sup>3</sup>
Effective volume of 1 chloride ion	$v_{Cl^-(2N)}$	$3.2928 \times 10^{-23} cm^3$

**Table 2.** Values of the parameters used to calculate the effective volume of chloride ions.

404

405 We can calculate the effective volume of chloride ions when the concentration is 2 N, as shown

406 in equation (16):

407  $v_{Cl^-(2N)} \cong 3.966 cm^3 / (0.2 \times N_0) = 3.966 / (0.2 \times 6.02214 \times 10^{23}) = 3.2928 \times$

408  $10^{-23} cm^3 \dots \dots \dots$  (16)

409 where  $v_{Cl^-(2N)}$  is the effective volume of chloride ions at a concentration of 2 N and  $N_0 =$

410  $6.02214 \times 10^{23}$ . <sup>10</sup>

411

412 2.1.5.2. Calculation of the net mass of chloride ( $Cl^-$ ) ions

413 The values of the parameters used to calculate the net mass of chloride ions are

414 summarized in Table 3.

415

Parameter	Symbol	Value
Density of the solution after 2 N KCl is dissolved in one kilogram of water at $25^\circ C$ , <sup>16</sup>	$d_{KCl(2N)+1kgH_2O}$	$1.08166 g/cm^3$
net mass of chloride ions	$m_{Cl^-.net}$	$2.3252 \times 10^{-26} kg$

**Table 3.** Values of the parameters used to calculate the net mass of chloride ions.

416

417 The buoyancy of the ions can be subtracted to obtain the net mass. From equation (15),

418 the net mass of chloride ions at a concentration of 2 N can be calculated as equation (17).

419  $m_{Cl^-.net} = m_{Cl^-} - v_{Cl^-(2N)} \times d_{KCl+1kgH_2O} = (35.446 g + 35.457 g)/2/N_0 -$

420  $(1.08166 g/cm^3) \times (3.2928 \times 10^{-23} cm^3) = 2.3252 \times 10^{-23} g = 2.3252 \times$

421  $10^{-26} kg \dots \dots \dots (17)$

422

423 2.1.5.3. Calculation of the effective volume of potassium ( $K^+$ ) ions

424 The density of a potassium chloride aqueous solution can be used to calculate the volume

425 of potassium ions plus chloride ions, after which the volume of chloride ions can be subtracted to

426 obtain the volume of potassium ions. The values of the parameters used to calculate the effective

427 volume of potassium ( $K^+$ ) ions are summarized in Table 4.

428

Parameter	Symbol	Value
Mass of KCl in one mole <sup>11</sup>	$W_{mol.KCl}$	74.550 g
Density of the solution after 2 N KCl is dissolved in one kilogram of water at 25°C, <sup>16</sup>	$d_{KCl(2N)+1kgH2O}$	1.08166 g/cm <sup>3</sup>
Density of the solution after 1.8 N KCl is dissolved in one kilogram of water at 25°C. <sup>16</sup>	$d_{KCl(1.8N)+1kgH2O}$	1.07390 g/cm <sup>3</sup>
Volume of the solution after 2 N KCl is dissolved in one kilogram of water at 25°C. ( $V = W/d$ )	$V_{KCl(2N)+1kgH2O}$	1062.349 cm <sup>3</sup>
Volume of the solution after 1.8 N KCl is dissolved in one kilogram of water at 25°C. ( $V = W/d$ )	$V_{KCl(1.8N)+1kgH2O}$	1056.141 cm <sup>3</sup>
Effective volume of 0.2 mole $K^+$ + 0.2 mole $Cl^-$ in a 2 N HCl solution	$0.2(V_{K^+(2N)} + V_{Cl^-(2N)})$	6.207 cm <sup>3</sup>
Effective volume of 1 mol chloride ions <sup>table.3.</sup>	$V_{Cl^-(2N)}$	19.83 cm <sup>3</sup>
Effective volume of 1 mol potassium ions	$V_{K^+(2N)}$	11.205 cm <sup>3</sup>
Effective volume of 1 potassium ion	$v_{K^+(2N)}$	$1.8608 \times 10^{-23} cm^3$

**Table 4.** Values of the parameters used to calculate the effective volume of potassium ions.

430

431 We can calculate the effective volume of potassium ions when the concentration is 2 N,

432 as shown in equation (18):

433 
$$v_{K^+(2N)} \cong 2.241 cm^3 / (0.2 \times N_0) = 2.241 / (0.2 \times 6.02214 \times 10^{23}) = 1.8608 \times$$

434 
$$10^{-23} cm^3 \quad \dots \dots \dots \quad (18)$$

435 where  $v_{K^+(2N)}$  is the effective volume of potassium ions at a concentration of 2 N and  $N_0 =$ 

436  $6.02214 \times 10^{23}$ . <sup>10</sup>

437

438 2.1.5.4. Calculation of the net mass of potassium ( $K^+$ ) ions

439 The values of the parameters used to calculate the net mass of potassium ions are  
 440 summarized in Table 5.

441

Parameter	Symbol	Value
Density of the solution after 2 N KCl is dissolved in one kilogram of water at $25^\circ C$ , <sup>16</sup>	$d_{KCl(2N)+1kgH_2O}$	$1.08166 g/cm^3$
net mass of potassium ions	$m_{K^+.net}$	$4.4797 \times 10^{-26} kg$

**Table 5.** Values of the parameters used to calculate the net mass of potassium ions.

442

443 The buoyancy force on potassium ions can be calculated from the volume of potassium  
 444 ions, and the net mass of potassium ions can be calculated. From equation (18), the net mass of  
 445 potassium ions at a concentration of 2 N can be calculated as equation (19).

446  $m_{K^+.net} = m_{K^+} - v_{K^+(2N)} \times d_{KCl+1kgH_2O} = (39.0983 g)/N_0 - (1.08166 g/cm^3) \times$   
 447  $(1.8608 \times 10^{-23} cm^3) = 4.4797 \times 10^{-23} g = 4.4797 \times 10^{-26} kg \quad \dots \dots \dots \quad (19)$

448 A comparison of equations (18) and (19) clearly reveals that the net mass difference  
 449 between chloride ions and potassium ions in aqueous solution is substantial. This makes the  
 450 gravitational effect more pronounced, thus making potassium chloride solution an excellent  
 451 medium for studying this phenomenon.

452

453 2.1.5.5. Calculation of the concentration variations of chloride ( $Cl^-$ ) and potassium ( $K^+$ ) ions

454 Assuming that the concentrations of chloride ions and potassium ions at zero height are  
 455 both 2 N. Referring to equations (13), (14), (17), and (19), the changes in the chloride ion  
 456 concentration and potassium ion concentration with height under the steady state without

457 convection can be obtained as shown in Fig. 2, where the vertical axis in the figure represents the  
458 concentration value and the horizontal axis represents the height value.  
459

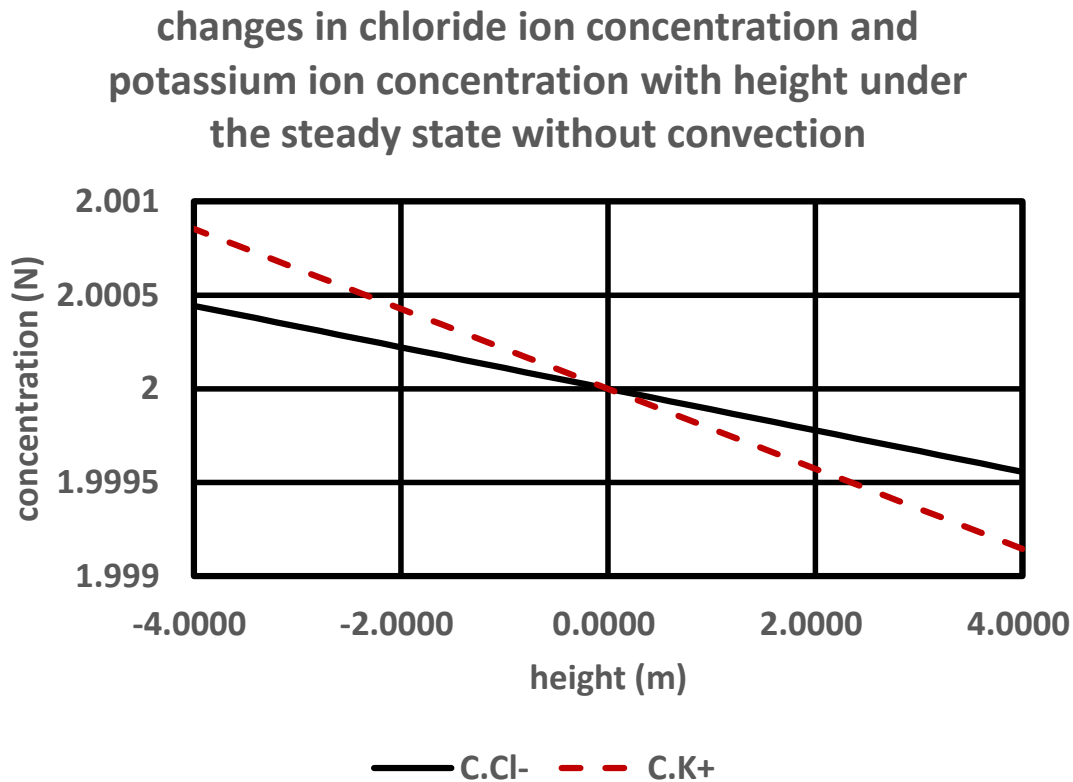


**Fig. 2.** The concentrations of chloride ions and potassium ions at zero height are both 2 N, and the changes in the chloride ion concentration and potassium ion concentration with height are under the steady state without convection. The vertical axis is the concentration value in N, and the horizontal axis is the height value in m.

460

#### 461 2.1.6. Changes in the pH of the Aqueous Solution with Height under Gravity

462 In salt solutions with a pH close to 7, even slight variations in the concentration of  
463 positive or negative ions can lead to significant changes in the pH value, which in turn affect the  
464 chemical potential of the solution. Therefore, when the pH of salt solutions is adjusted to near 7,



465 gravity or centrifugal forces only need to cause minimal shifts in ion concentrations to produce  
 466 notable voltage variations. Consequently, investigating the effects of gravity or centrifugal forces  
 467 on ion concentrations in salt solutions with a pH close to 7 is crucial, as voltage changes in this  
 468 range are both significant and easily detectable. A potassium chloride aqueous solution with a  
 469 concentration of 2 N was used as an example.

470 Because chloride ions and potassium ions are both strong electrolytes, they are almost  
 471 completely dissociated. Because the total charge of ions in aqueous solution is close to zero,  
 472 equation (20) can be derived.

$$473 \quad [C_{OH^-}] + [C_{Cl^-}] = [C_{K^+}] + [C_{H^+}] \quad \dots \dots \dots \quad (20)$$

474 where  $[C_{OH^-}]$  is the hydroxide ion concentration,  $[C_{Cl^-}]$  is the chloride ion concentration,  $[C_{K^+}]$   
 475 is the potassium ion concentration, and  $[C_{H^+}]$  is the hydrogen ion concentration.

476 From the equilibrium concentration relationship equation (21)<sup>17</sup> between hydrogen ions  
 477 and hydroxide ions at 25°C and combined with equation (20), equations (22) and (23) can be  
 478 deduced.

$$479 \quad [C_{H^+}][C_{OH^-}] = 1.008 \times 10^{-14} \quad \dots \dots \dots \quad (21)$$

$$480 \quad \Rightarrow ([C_{K^+}] - [C_{Cl^-}] + [C_{H^+}])[C_{H^+}] = 1.008 \times 10^{-14}$$

$$481 \quad [C_{H^+}]^2 + [C_{H^+}]([C_{K^+}] - [C_{Cl^-}]) = 1.008 \times 10^{-14}$$

$$482 \quad \left( [C_{H^+}] + \frac{1}{2}[C_{K^+}] - \frac{1}{2}[C_{Cl^-}] \right)^2 = 1.008 \times 10^{-14} + \frac{1}{4}([C_{K^+}] - [C_{Cl^-}])^2$$

$$483 \quad [C_{H^+}] = \sqrt{1.008 \times 10^{-14} + \frac{1}{4}([C_{K^+}] - [C_{Cl^-}])^2} - \frac{1}{2}([C_{K^+}] - [C_{Cl^-}]) \quad \dots \dots \dots \quad (22)$$

$$484 \quad pH = -\log[C_{H^+}] = -\log \left( \sqrt{1.008 \times 10^{-14} + \frac{1}{4}([C_{K^+}] - [C_{Cl^-}])^2} - \frac{1}{2}([C_{K^+}] - [C_{Cl^-}]) \right)$$

$$485 \quad \dots \dots \dots \quad (23)$$

486 Substituting the previously calculated results shown in Fig. 2 into equation (23), it can be  
487 seen that after standing under gravity for a long time, the change in pH with height will be as  
488 shown below (Fig. 3):

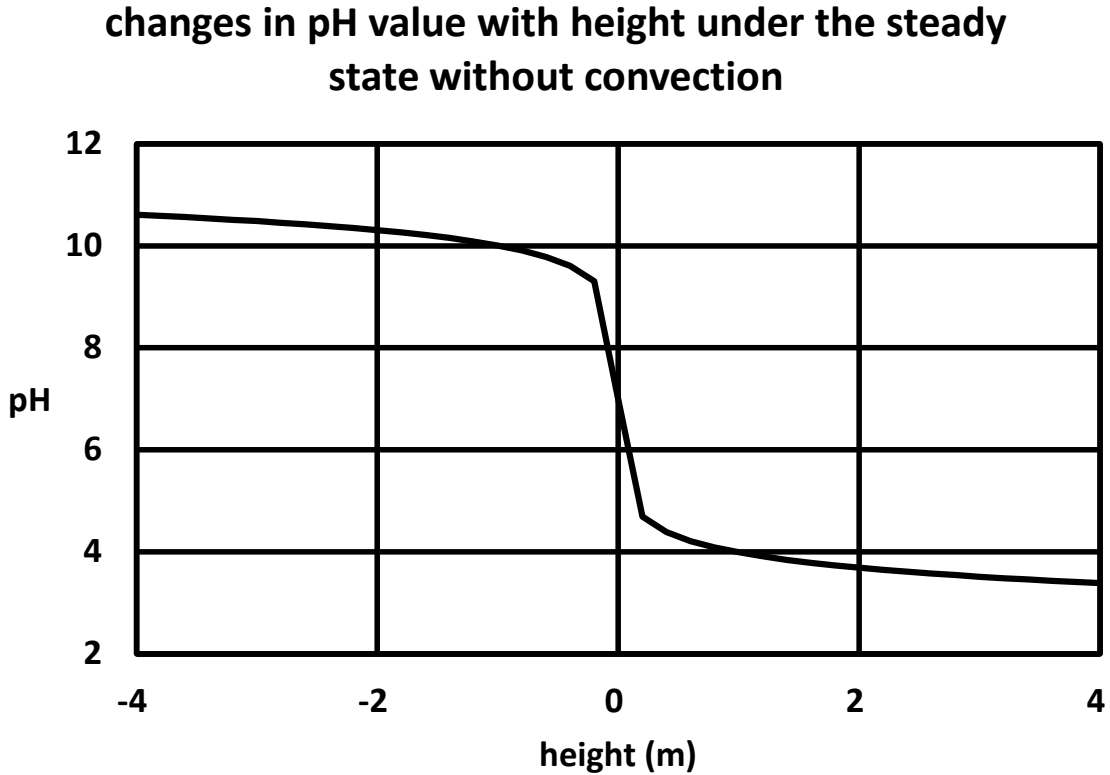


**Fig. 3.** The calculated pH value of the KCl aqueous solution at equilibrium. The vertical axis represents the pH value, and the horizontal axis represents the height in m.

489  
490 As shown in Figure 3, the change in pH with height is nonlinear, and thus, the voltage difference  
491 is also nonlinear. Consequently, if the acceleration or centrifugal force is increased by a factor of  
492 four, achieving a fourfold voltage difference requires dividing the height into four equal parts. In  
493 this way, one quarter of the original height will exhibit the original voltage difference. By

494 stacking and electrically connecting these four sections in series, it is possible to obtain four  
495 times the voltage difference within the same space or height.

496

### 497 *2.1.7. Changes in the Voltage of the Aqueous Solution with Height under a Gravity Field*

498 The chemical potential of aqueous solutions changes with pH. A previous inference was  
499 reached that the pH changes with height so that the chemical potential also changes with height.

500 The relationship between the voltage change and concentration can be obtained from the Nernst  
501 equation,<sup>18</sup> such as equation (24).

$$502 \quad \Delta V = -\frac{RT}{nF} \ln \left( \frac{[C]}{[C]_0} \right) \quad \dots \dots \dots \quad (24)$$

503 where  $\Delta V$  is the voltage difference from the reference concentration,  $[C]$  is the concentration,  
504  $[C]_0$  is the reference concentration,  $n$  is the number of electrons exchanged in the reaction,  $F =$   
505  $69485.333 \text{ C/mol}$  is Faraday's constant,<sup>10</sup>  $R = 8.31446 \text{ J/(mol} \times \text{K)}$  is the universal gas  
506 constant,<sup>10</sup> and  $T$  is the absolute temperature. For positively charged hydrogen ions and  
507 potassium ions,  $n=1$ ; for negatively charged hydroxide ions and chloride ions,  $n=1$ .

508 Using the data previously calculated and shown in Fig. 2 and formulas (21) and (22),  
509 Figs. 4 and 5 can be obtained. Fig. 4 shows the relationship between the electrode potential  
510 difference and height when the electrode exchanges electrons with potassium ions or chloride  
511 ions. Fig. 5 shows the relationship between the electrode potential difference and height when  
512 the electrode exchanges electrons with hydrogen ions or hydroxide ions. Figure 4 shows that  
513 when interfacial reactions involve charge exchange with potassium ions, the voltage decreases  
514 with increasing height; that is, the voltage increases along the direction of the applied force field  
515 (FF). Figures 4 and 5 show that when the electrode exchanges electrons with chloride ions,

516 hydrogen ions, or hydroxide ions, the voltage increases with height; in other words, the voltage  
517 increases in the direction opposite to the force field.

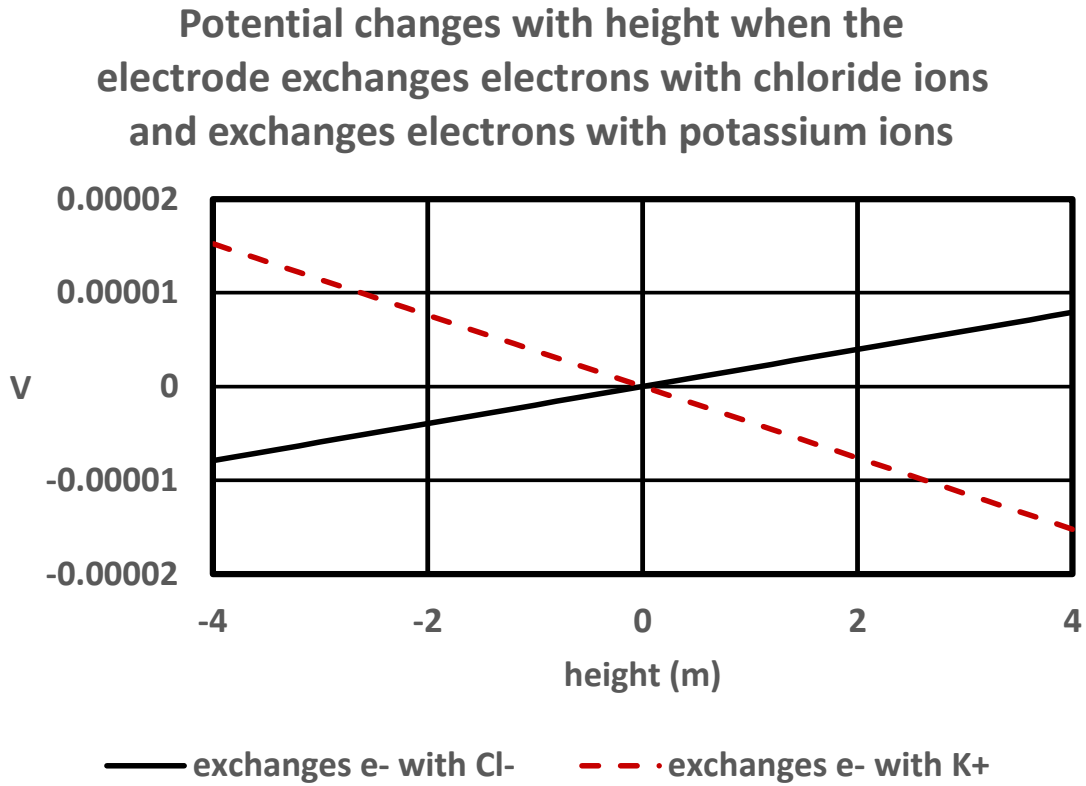


**Fig. 4.** The potential changes with height when the electrode exchanges electrons with chloride ions and exchanges electrons with potassium ions.

### The change in potential with height when the electrode exchanges electrons with hydrogen ions or hydroxide ions

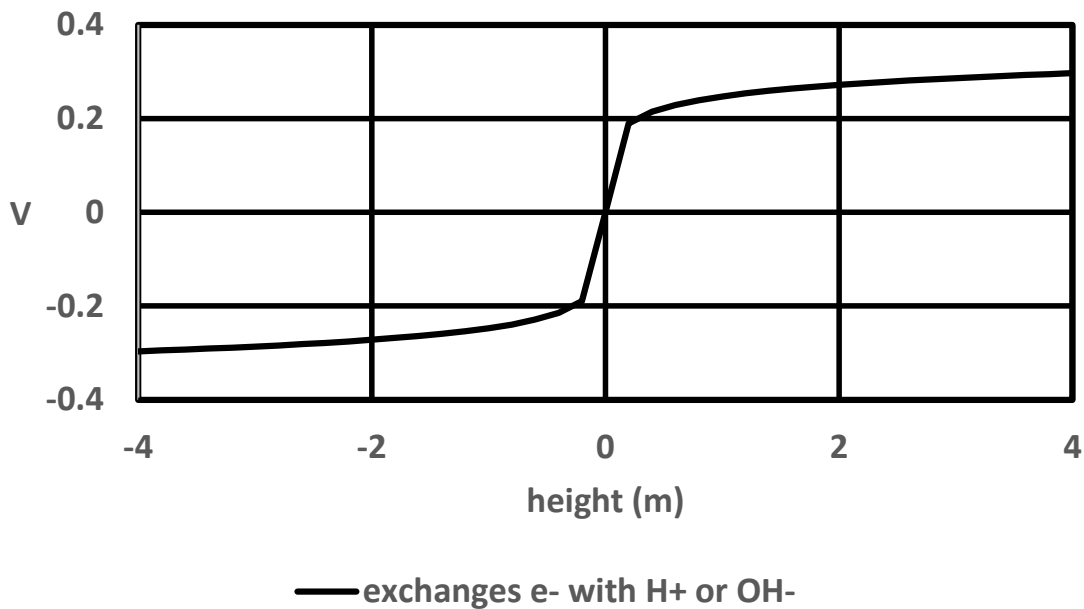


**Fig. 5.** The change in potential with height when the electrode exchanges electrons with hydrogen ions or hydroxide ions.

518

519           The lower the pH is, the higher the concentration of hydrogen ions, and the opposite is  
520 true for hydroxide ions. Fig. 3 shows that the concentration of hydrogen ions is greater at high  
521 positions, and the concentration of hydroxide ions is greater at low positions. When the upper  
522 and lower ends are connected to a resistor, the resistor links the two ends, altering the voltage  
523 and causing the ion concentrations to deviate from equilibrium, thus initiating diffusion. In this  
524 process, the hydrogen ions above diffuse downward, whereas the hydroxide ions diffuse upward,  
525 meeting and combining in the central area to form water. This is similar to what occurs in  
526 plasma, where the diffusion energy of atoms and ions is also derived from the thermal energy of  
527 thermal vibrations. The downward movement of positively charged hydrogen ions and the

528 upward movement of negatively charged hydroxide ions can both create internal currents from  
529 top to bottom, thus forming a gravity battery that outputs electrical energy through an external  
530 resistor. Similarly, when positively charged potassium ions and negatively charged chloride ions  
531 diffuse upward or downward, an electric current is also generated. Therefore, the energy is sent  
532 out without a temperature difference.

533         The above discussion theoretically examines the changes in concentration and electric  
534 field within plasma or ionic solutions under the influence of gravitational or centrifugal forces,  
535 essentially in the presence of acceleration. The following section describes our experimental  
536 approach to validate this phenomenon and how we measured continuous and stable current  
537 outputs in the absence of a temperature difference.

538

## 539 **2.2. Experimental Verification**

540

### 541 *2.2.1. Experimental Procedure*

542         To assess the impact of gravity on the ion concentration and electrical potential in  
543 potassium chloride (KCl) solutions, we designed a set of gravity cells using titanium electrode  
544 sheets coated with platinum. Titanium was chosen for its chemical inertness, preventing any  
545 unwanted reactions with the KCl solution. Each electrode sheet had a diameter of 50 mm and  
546 was coated with 1  $\mu\text{m}$  of platinum on both sides.

547         Silicone rings, with an inner diameter of 40 mm and an outer diameter of 60 mm, were  
548 used to create cavities to hold the ionic aqueous solution. The silicone rings were carefully  
549 selected to avoid any chemical reactions with the solution. Each cavity was equipped with a  
550 silicone tube to facilitate filling with the KCl solution. The overall design of the cell, including

551 the assembly of multiple layers separated by silicone rings of varying thicknesses (2 mm to 32  
552 mm), allowed for a series of electrical connections across the chambers. The arrangement is  
553 depicted in Figure 6.

554 The theoretical derivation suggested that the largest voltage change occurs when the pH  
555 is close to 7. Therefore, a 2 N KCl aqueous solution with a pH near 7 was prepared through  
556 vacuum degassing, which minimizes gas bubbles that could otherwise obstruct potential  
557 conduction or current flow. However, vacuum degassing also poses the risk of altering the pH by  
558 removing trace amounts of chlorine gas. Two gravity cells with different degassing durations  
559 were prepared. The longer degassing time of one cell led to a slight reduction in the chloride ion  
560 concentration due to chlorine gas removal.

561 Once prepared, the degassed KCl solution was injected into each cavity of the gravity  
562 cells, and the openings were sealed. The electrode connections were then completed, as shown in  
563 the center panel of Figure 6, with the internal structure displayed in Figure 7. Epoxy resin was  
564 used to seal the assembled cells within stainless steel casings to prevent deformation or leakage  
565 during high-centrifugal force experiments.

566 The gravity cells were placed into a centrifuge with a rotation radius of 1200 mm and  
567 balanced by placing them opposite one another to maintain a stable center of gravity. The  
568 experimental setup included an MMV-387SD voltage recorder positioned at the center of the  
569 centrifuge. The centrifuge was operated at 10 G (ten times Earth's gravity) for two hours, during  
570 which the voltage output was continuously monitored. This duration allowed sufficient diffusion  
571 time for the solution to reach a near-equilibrium ion concentration gradient, confirming that a  
572 voltage difference can be generated under high centrifugal force.

573 After the centrifugal force measurements, the cells were allowed to rest for 30 minutes,  
574 during which the discharge process was recorded, demonstrating that the voltage difference  
575 disappears once the centrifugal force is removed.

576 To fully discharge the gravity cells and remove any residual charge, they were short-  
577 circuited and left horizontally for 290 days (with gravity parallel to the electrode plates). 為 The  
578 samples were subsequently placed vertically (gravity perpendicular to the electrode plates) for  
579 three days to allow the ion distribution to stabilize under gravity, as shown in the left panel of  
580 Figure 8. The stabilized voltage was then measured via a KEYSIGHT34465A meter. To avoid  
581 electromagnetic interference, the setup was enclosed in an iron cabinet during the measurements.

582 In previous experiments, the voltage was measured with no current flow. To determine  
583 whether a continuous current output could be sustained over time, a 6.8 MΩ resistor was  
584 connected across the electrodes of the vertically placed gravity cell. The voltage was measured  
585 six times between the 15th and 55th days.

586 To test whether gravity truly caused the observed potential difference, the cells were  
587 inverted, allowing the solution to stabilize for 86 days. Voltage measurements were taken 24  
588 times between the 33rd and 86th days, with the expectation that the inverted configuration would  
589 yield opposite voltage and current values.

590





**Fig. 6.** Selected images of the gravity battery production process.

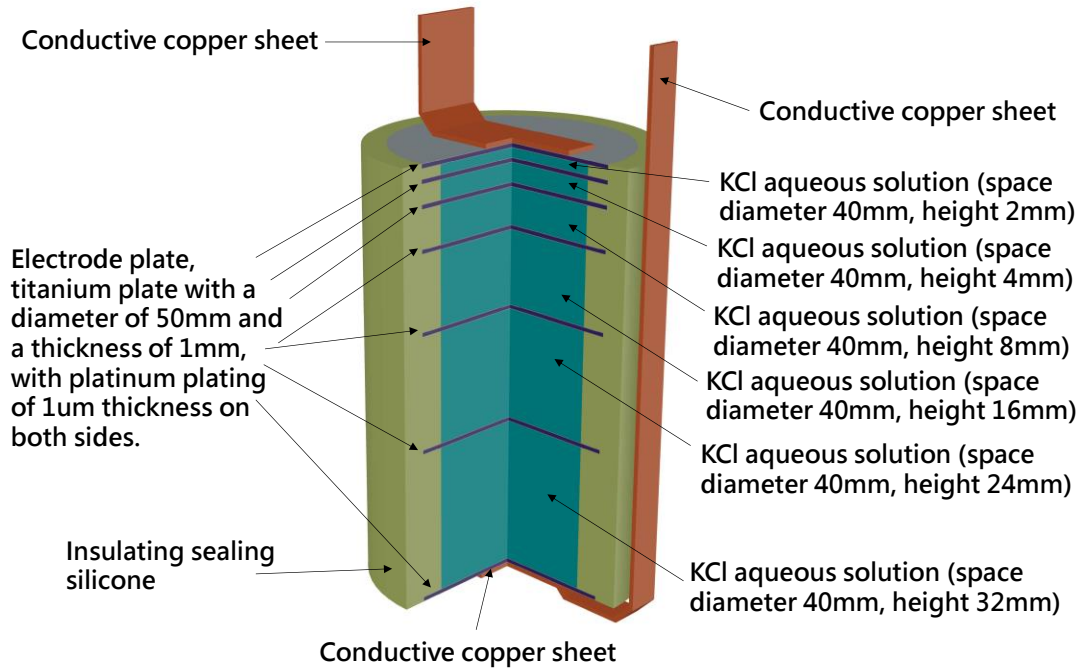


**Fig. 7.** Internal structure diagram of the gravity battery, including six small units with electrode spacings of 32 mm, 24 mm, 16 mm, 8 mm, 4 mm, and 2 mm that are electrically connected in series.



**Fig. 8.** Selected images of the gravity battery during the static measurement process.

591

### 592 2.2.2. Experimental Results

593 The left panel of Figure 9 shows the experimental setup, whereas the right panel illustrates the  
594 relationship between the output voltage and time under a 10 G centrifugal force field. As the 10G  
595 field was applied, the voltage difference between the two gravity batteries gradually increased,  
596 confirming that the centrifugal force induced potential changes in the solution along the direction  
597 of the field. This suggests that the device can continuously convert ambient thermal energy into  
598 electrical energy when exposed to a sufficiently large gravitational or centrifugal force. Small  
599 differences in pH between the two gravity batteries led to variations in the timing and magnitude  
600 of the generated potentials. Once the centrifuge stopped and no centrifugal force was applied, the  
601 potential quickly returned to its initial state.

602

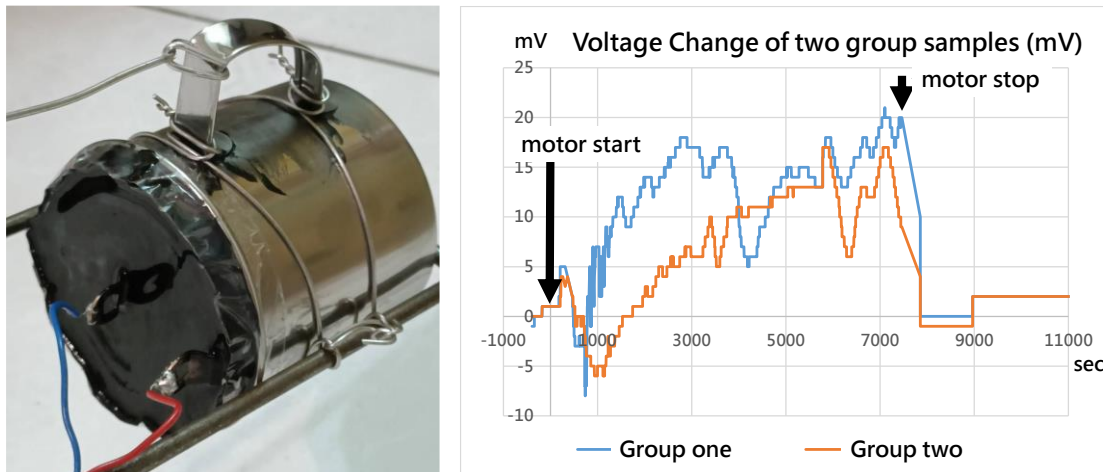


**Fig. 9.** The gravity battery unit was subjected to a centrifugal force field of 10 G (10 times the gravity of the Earth's surface), and the output voltage was continuously recorded for two hours. The resulting relationship between the measured potential and time is shown.

603

604 Table 6 summarizes the voltage measurements from the first and second samples when  
605 placed vertically with a 6.8 MΩ load from a resistor. The first sample exhibited an average

606 output voltage of 22.594 mV with a standard deviation of 3.240 mV over 40 days (15<sup>th</sup> to 55<sup>th</sup>),  
 607 whereas the second sample had an average output voltage of -0.647 mV with a standard  
 608 deviation of 0.503 mV. Individual measurements for both samples are listed in the table.  
 609

Sample	Day 15	Day 25	Day 34	Day 41	Day 48	Day 55
1st	26.460 mV	25.571 mV	22.611 mV	19.423 mV	23.181 mV	23.181 mV
2nd	-0.331 mV	-0.123 mV	-0.272 mV	0.750 mV	-0.959 mV	-0.959 mV
Sample	Mean	Standard Deviation				
1st	22.594 mV	3.240 mV				
2nd	-0.647 mV	0.503 mV				

**Table 6.** Voltage measurements from the first and second samples when placed vertically with a 6.8 MΩ load from a resistor.

610

611 The data before the 15th day were discarded because the measurements taken before the  
 612 15th day were taken when the probe was in direct contact with the contacts of the gravity battery,  
 613 so a small vibration would occur when the connection was made. This small vibration will cause  
 614 turbulence in the electrolyte and destroy the stable state. After the 15th day, we switched to using  
 615 fixed wires to connect to the electrodes of the gravity battery, and the probe was only in contact  
 616 with the other end of the wire to eliminate the impact of vibration on the measurement. During  
 617 the measurement process, we only used the first result, which was measured after the participants  
 618 had stood for a whole night. When people move around the laboratory, the gas heated by a  
 619 person's body temperature affects the ambient temperature, which flows through and contacts the  
 620 gravity battery. This causes slight convection in the ionic aqueous solution in the gravity battery,  
 621 causing it to deviate from the stable state.

622 To confirm that the potential difference is due to gravity, the opposite voltage should be  
 623 measured when the gravity cell is turned upside down. When the same samples were placed  
 624 upside down, the voltage began to change. The average output voltage of the first sample from  
 625 the 33rd day to the 86th day was -4.169 mV, and the measurement standard deviation was 1.396  
 626 mV; the average output of the second sample was 11.148 mV, and the measurement standard  
 627 deviation was 0.282 mV.

628 Table 7 summarizes the voltage measurements from the first and second samples when  
 629 placed upside down with a 6.8 MΩ load from a resistor.

630

Sample	Day 33	Day 35	Day 37	Day 39	Day 41	Day 44
1st	-2.113 mV	-1.149 mV	-1.895 mV	-2.476 mV	-2.028 mV	-2.928 mV
2nd	11.702 mV	11.496 mV	11.241 mV	11.189 mV	10.871 mV	10.938 mV
Sample	Day 46	Day 48	Day 51	Day 53	Day 55	Day 58
1st	-5.729 mV	-6.162 mV	-5.669 mV	-4.141 mV	-3.860 mV	-4.732 mV
2nd	11.311 mV	10.733 mV	11.718 mV	11.302 mV	11.345 mV	11.244 mV
Sample	Day 60	Day 62	Day 65	Day 67	Day 69	Day 72
1st	-4.320 mV	-5.309 mV	-4.546 mV	-4.727 mV	-4.489 mV	-4.878 mV
2nd	11.362 mV	11.167 mV	10.909 mV	11.049 mV	11.215 mV	11.040 mV
Sample	Day 74	Day 76	Day 79	Day 81	Day 83	Day 86
1st	-4.066 mV	-4.959 mV	-4.295 mV	-6.263 mV	-5.091 mV	-4.234 mV
2nd	11.193 mV	11.204 mV	10.901 mV	11.064 mV	10.771 mV	10.577 mV
Sample	Mean	Standard Deviation				
1st	-4.169 mV	1.396 mV				
2nd	11.148 mV	0.282 mV				

**Table 7.** Voltage measurements from the first and second samples when placed upside  
 down with a 6.8 MΩ load from a resistor.

631

632           The measurement results show that the output voltages of the upright and upside-down  
633 devices are opposite. Moreover, the voltage directions of the two samples are different when they  
634 are standing. According to our previous theoretical calculations, when the electrode exchanges  
635 electrons with different ions or when the pH is different, the voltage difference will be different  
636 and may be opposite.

637           In centrifugal force experiments, a voltage bias is generated because of the presence of a  
638 centrifugal force and disappears when the centrifugal force is removed, leading to the conclusion  
639 that the centrifugal force is responsible for the potential difference. In experiments directly  
640 utilizing Earth's gravity, stable current and electrical energy output were maintained regardless of  
641 whether the system was placed upright or inverted, indicating that this voltage difference is not  
642 limited to a temporary state but represents a stable, steady condition. These experiments  
643 demonstrate that continuous energy conversion occurs in both gravitational and centrifugal force  
644 fields. According to the law of conservation of energy and supported by earlier theoretical  
645 derivations, the energy source is identified as the thermal energy from the environment. Our  
646 measurements are consistent with the phenomenon observed by T. Dale Stewart and Richard C.  
647 Tolman in 1910. <sup>4</sup>

648

### 649 **3. DISCUSSION**

650           When a force acts on the same physical properties of ions, since the ions move in a  
651 random and scattered manner, it must comply with Carnot's theorem,<sup>1</sup> which states that the  
652 maximum energy output rate of a heat engine cannot be greater than the temperature difference  
653 divided by the absolute temperature. However, when an electric field affects the charge of an ion,  
654 gravity affects the mass of the ion. The forces experienced by ions with different masses are

655 unequal, imparting directional characteristics to ion motion. This article raises the question of  
656 whether, in cases where ions of different masses exhibit diverse directional tendencies, it might  
657 be possible to surpass the constraints imposed by Carnot's theorem. <sup>1</sup> In our theoretical  
658 derivation, a potential difference caused by gravity is indeed derived. Therefore, it is possible to  
659 convert thermal energy into electrical energy without a temperature difference.

660 Although the initial theoretical derivations were based on plasma, practical experiments with ion  
661 plasma are challenging because ion plasma extraction is difficult to perform via centrifugation;  
662 therefore, we opted instead to conduct experiments using aqueous ion solutions with ions of  
663 different masses or mass–charge ratios. The first aqueous ion solution to be considered is sodium  
664 chloride, which is the easiest to obtain. Chloride ions and sodium ions have the same charge and  
665 opposite electrical properties, and the ion masses greatly differ, so they may be good  
666 experimental objects. However, when the buoyancy force on the effective volume in solution is  
667 considered, because the volume of chloride ions is much larger than that of sodium ions, after the  
668 buoyancy force is deducted, the net masses of the two ions will be very close, so observing the  
669 voltage difference due to gravity is difficult. Therefore, we changed the solution to a potassium  
670 chloride aqueous solution with similar original masses of positive and negative ions but a large  
671 difference in effective volume. As we calculated in the previous article, there is a large  
672 difference in the net masses of chloride ions and potassium ions. In the experiment, the potential  
673 difference was indeed measured when the sample was placed upright and upside down. That is,  
674 the same sample will have different potential differences in different directions of gravity. It can  
675 also be inferred that the voltage difference is caused by gravity.

676         In limited measurements, the voltage and current that can be measured are very small, but  
677 it can still be proven that thermal energy is converted into electrical energy without a

678 temperature difference. To amplify the energy output, a faster rotating centrifuge can be used. As  
679 mentioned in the article, for the same rotation radius and the same amount of electrolyte, when  
680 the rotation speed is doubled, appropriate structural modifications can produce sixteen times the  
681 output, whereas the energy lost to air resistance increases by only approximately four times.  
682 Therefore, increasing the rotational speed must increase the electrical energy output more than  
683 the energy lost to air resistance. In terms of energy conversion efficiency. Potassium chloride is  
684 not the most energy-efficient combination of ingredients, but many other chemical combinations  
685 could be tested.

686

#### 687 **4. CONCLUSION**

688 Energy conversion is crucial for the sustainable operation of our planet. While  
689 concentration cells have been extensively studied and applied, the potential difference caused by  
690 concentration gradients resulting from gravity or centrifugal force has not received sufficient  
691 attention. With the insight provided by Richard C. Tolman's 1910 observation of voltage bias in  
692 conductors within an accelerated force field, it becomes clear that such forces can indeed  
693 generate a potential difference<sup>4</sup>. Our theoretical calculations confirm that this potential difference  
694 occurs not only on the surface of the conductor but also within its interior, further suggesting that  
695 thermal energy can be converted into electrical energy even in the absence of a temperature  
696 difference. We demonstrated this experimentally by using a centrifugal force or artificial gravity  
697 to generate a potential difference. Furthermore, by utilizing natural gravity, we achieve a  
698 continuous current output. The reversal of the output voltage when the device is inverted further  
699 verifies that gravity can indeed produce a voltage difference and current.

700           This study concludes that, in the absence of a temperature gradient, the use of gravity or a  
701 centrifugal force provides a feasible method for converting thermal energy into electrical energy,  
702 thereby overcoming the limitations imposed by Carnot's theorem. <sup>1</sup> Although the mechanism for  
703 counteracting changes in ion concentration still requires further study, this approach holds  
704 promise as a viable green energy source. This discovery opens new avenues for research and  
705 practical applications in various directions.

706

#### 707 **ACKNOWLEDGMENTS**

708 We would like to acknowledge the professional manuscript services of American Journal  
709 Experts.

710

711

#### 712 **DATA AVAILABILITY STATEMENT**

713 Not applicable

714

#### 715 **DECLARATIONS**

716

#### 717 **Conflict of interest statement**

718 The author has no conflicts of interest to disclose.

719

#### 720 **Author Contributions**

721 Kuo Tso Chen designed the study, performed the experiments, analyzed the data, and wrote the  
722 manuscript.



723

724 **Ethics Approval**

725 I confirm that the manuscript has been approved by the author for publication. I declare that the  
726 work described herein is original research and that it has not been published previously.

727

728

729 **REFERENCES**

- 730 <sup>1</sup>Y. Izumida, "Irreversible efficiency and Carnot theorem for heat engines operating with  
731 multiple heat baths in linear response regime," *Phys. Rev. Res.* 4, 023217 (2022).
- 732 <sup>2</sup>M. R. Morad, F. Momeni, "On the proof of the first Carnot theorem in thermodynamics," *Eur. J.*  
733 *Phys.* 34, 1581–1588 (2013).
- 734 <sup>3</sup>Milivoje M. Kostic, "The Second Law and Entropy Misconceptions Demystified", *Entropy*  
735 2020, 22(6), 648 (2020), <https://www.mdpi.com/1099-4300/22/6/648> , Accessed 13  
736 November 2024.
- 737 <sup>4</sup>R.C. Tolman, "The Electromotive Force Produced in Solutions by Centrifugal Action", *Proc.*  
738 *Am. Acad. Arts Sci.* 46, 109 (1910),
- 739 <sup>5</sup>R. C. Tolman, and T. D. Stewart, "The electromotive force produced by the acceleration of  
740 metals," *Phys. Rev.* 8, 97–116 (1916).
- 741 <sup>6</sup>Colley, R., "Nachweis der Existenz der Maxwellschen electromotorischen Kraft". *Wiedemann's*  
742 *Annalen der Physik*, 17, 55-70.(1882)
- 743 <sup>7</sup>Des Coudres, Th., "Nachweis der Existenz der Maxwellschen electromotorischen Kraft".  
744 *Annalen der Physik*, 49, 284-300.(1893).
- 745 <sup>8</sup>L. Lao, C. Ramshaw, H. Yeung, "Process intensification: water electrolysis in a centrifugal  
746 acceleration field", *Journal of Applied Electrochemistry*, 41, 645-656, (2011).  
747 <https://link.springer.com/article/10.1007/s10800-011-0275-2>.
- 748 <sup>9</sup>J. W. Gibbs, *Elementary Principles in Statistical Mechanics* (Charles Scribner's Sons, 1902).
- 749 <sup>10</sup>P. J. Mohr, D. B. Newell, and B. N. Taylor, "2014 CODATA recommended values of the  
750 fundamental constants of physics and chemistry," (2014), Accessed 8 June 2023,  
751 [https://physics.nist.gov/cuu/pdf/wallet\\_2014.pdf](https://physics.nist.gov/cuu/pdf/wallet_2014.pdf).
- 752 <sup>11</sup>T. Prohaska, J. Irrgeher, J. Benefield, J. K. Böhlke, L. A. Chesson, T. B. Coplen, T. Ding, P. J.  
753 H. Dunn, M. Gröning, N. E. Holden, H. A. J. Meijer, H. Moossen, A. Possolo, Y.  
754 Takahashi, J. Vogl, T. Walczyk, J. Wang, M. E. Wieser, S. Yoneda, X.-K. Zhu, and J.  
755 Meija, "Standard atomic weights of the elements 2021 (IUPAC Technical Report)," *Pure*  
756 *Appl. Chem.* 94, 573–600 (2022).
- 757 <sup>12</sup>P. J. Mohr, D. B. Newell, and B. N. Taylor, *CODATA Recommended Values of the*  
758 *Fundamental Physical Constants: 2014* (National Institute of Standards and Technology,  
759 2015).
- 760 <sup>13</sup>O. G. Simon, *The Galvanic Circuit Investigated Mathematically* (D. Van Nostrand Company,  
761 1891).
- 762 <sup>14</sup>B. N. Taylor, and A. Thompson, *The International System of Units (SI), NIST Special*  
763 *Publication 330 2008 Edition* (National Institute of Standards and Technology, 2008).
- 764 <sup>15</sup>D. Rowland, "Density of hydrochloric acid, HCl(aq), advanced thermodynamics," *Advanced*  
765 *Thermodynamics*, 2021, Accessed 8 June 2023,  
766 [https://advancedthermo.com/electrolytes/density\\_HCl.html](https://advancedthermo.com/electrolytes/density_HCl.html).
- 767 <sup>16</sup>D. Rowland, "Density of potassium chloride, KCl(aq), advanced thermodynamics," *Advanced*  
768 *Thermodynamics*, 2021, Accessed 8 June 2023,  
769 [https://advancedthermo.com/electrolytes/density\\_KCl.html](https://advancedthermo.com/electrolytes/density_KCl.html).
- 770 <sup>17</sup>J. Clark, "The ionic product for water, kw, acidbaseeqia, physical, chemguide," *Chemguide*,  
771 2014, Accessed 12 November 2023,  
772 <https://www.chemguide.co.uk/physical/acidbaseeqia/kw.html>.

773 <sup>18</sup>D. Larsen, "20.6: The Nernst equation1. Chemistry libretexts," (2016), Accessed 7 November  
774 2023,  
775 [https://chem.libretexts.org/Courses/Heartland\\_Community\\_College/HCC%3A\\_Chem\\_16](https://chem.libretexts.org/Courses/Heartland_Community_College/HCC%3A_Chem_162/20%3A_Electrochemistry/20.6%3A_The_Nernst_Equation)  
776 [2/20%3A\\_Electrochemistry/20.6%3A\\_The\\_Nernst\\_Equation](https://chem.libretexts.org/Courses/Heartland_Community_College/HCC%3A_Chem_162/20%3A_Electrochemistry/20.6%3A_The_Nernst_Equation).  
777